Suprathermal electrons in a stationary magnetic arc discharge

Ole Waldmann[1], Martin Langowski[2], and Gerd Fussmann[3]

[1]OWaldmann@lbl.gov, Lawrence Berkeley National Lab, 1 Cyclotron Road Mail Stop 5-121, Berkeley, CA 94720, USA, [2]Universität Bremen, Institut für Umweltphysik (IUP), Otto-Hahn-Allee 1, 28359 Bremen, Germany [3]Humboldt-Universität zu Berlin, Institut für Physik, Newtonstr. 15, 12489 Berlin, Germany

Abstract. Stochastic short voltage spikes occur in the stationary arc discharge of the linear plasma generator PSI-2. Similar spikes are also found when detecting the infrared bremsstrahlung emission at various plasma positions. They are related to suprathermal electrons which have energies up to 150 eV, i.e. 1.5 times the average discharge voltage and 15 times $k_\mathrm{B}T_\mathrm{e}$, the thermal energy of the bulk electrons.
These electrons are examined by different diagnostic methods, in particular a newly constructed segmented neutralizer plate was used as a diagnostic tool. The suprathermal particles are found to exist in a thin circular ring of the plasma column which is the region of field lines connected directly to the cathode.
For low neutral gas pressure the suprathermal electrons can be treated as collisionless, but when increasing the neutral gas background scattering with the molecules must be taken into account.
In some cases the peak in the potential of the collecting neutralizer plate exceeds the peak of the accelerating voltage. This is explained as a transient event occurring when a bunch of electrons is approaching the collecting surface.
The maximum current associated with these electrons is found to compensate the ion saturation current. Their peak density is thus estimated to be in the range of 10^{-3} of the thermal electrons; on temporal average the ratio $\langle n_\mathrm{st}\rangle/n_\mathrm{e}$ is of order 10^{-8}.
To our knowledge this is the first extensive study on suprathermal electrons in magnetized arcs. They provide an interesting physical phenomenon but are unlikely to affect the interpretation of electrical probes or optical diagnostic measurements.

PACS numbers: 52.25.Xz, 52.50.Nr, 52.70.Ds, 52.70.Kz

1. Introduction

In what follows we use the key word *suprathermals* to identify an overpopulation in the tails of the electron energy distribution function, which otherwise may still be be characterized by a Maxwellian $f(v) = f_\mathrm{M}(v)$ and a temperature T_e in an approximated manner. Such deviations from a Maxwellian are likely to occur in low density plasmas because of low collision rates. Furthermore, due to the well known relation $\nu_\mathrm{e} \sim v^{-2}$ of the collision frequency on velocity, the tail ($v \gg \sqrt{k_\mathrm{B}T_\mathrm{e}}$) of the distribution function is particularly susceptible to deviations from a Maxwellian whereas the core region

($v < \sqrt{k_\mathrm{B} T_\mathrm{e}}$) is much less affected.

The perhaps most prominent occurrence of suprathermals is the runaway phenomenon observed in tokamaks where a rather weak, stationary electric field causes a permanent acceleration of electrons, thereby producing relativistic particles. Less pronounced energy enhancements are to be expected in case of fluctuating electric fields or when the particles are exerted to the field only for a short time because of losses to the walls. Such a situation is met in the experiments described in this article where we report on deviations from a Maxwellian during short periods in a stationary arc discharge. Although the general performance of the plasma may be little influenced by the presence of the suprathermals in this case they can, nevertheless, play a crucial role with respect to certain aspects, like the excitation of high energy levels of atoms or ions and the corresponding emission of spectral lines. In addition, diagnostic methods relying on Maxwellion distributions for evaluation, like Langmuir probes and others, can fail and deliver in particular too high electron temperatures. Similarly, electrostatic plasma waves are likely to be excited on account of "bump in tail" instabilities. As a consequence the (micro wave) emission at the plasma frequency will be enhanced. It is therefore important to have at least an approximate knowledge of the number and the energy range of the suprathermals. Although the conditions prevailing in our experiment are specific and cannot give a general answer to other low density plasmas we think that the diagnostic methods and theoretical considerations applied may be helpful to assess the situation in other cases too.

As far as we know, no other papers have been published on this matter since our first publication in 2006 [1], but there are a number of articles that give indirect hints on suprathermal electrons in stationary linear devices such as Refs. [2, 3, 4, 5, 6, 7]. Most of these papers deal with the interpretation of spectral lines and how they may be influenced by a nonthermal population of electrons. They all show contradictions between theory and experiment regarding the electron temperature if the electron distribution functions are assumed to be purely Maxwellians. Therefore, the authors claimed the existence of suprathermal electrons without diagnosing them directly.

Despite the stationarity of the arc discharge in PSI-2, cf. Sec. 2, we find short spikes in the cathode-anode voltage. The mechanism by which these spikes are produced is not fully understood yet, but as discussed in Ref. [1], we presume that they are triggered by fluctuations in the electric field strength in front of the heated LaB_6 cathode. Once this extracting field is slightly reduced the emitted electron current tends to break down. This, however, is prevented by the inductance of the power supply (enhanced by a control system) that immediately rises the voltage to keep the current at a constant level.

The suprathermal electrons being produced during large voltage spikes are observed for any working gas and discharge regime but they are most prominent in hydrogen which is therefore the preferred working gas in this work. The particular role of hydrogen is likely to be found in the current-voltage characteristics ($I = I(U)$). In fact, the dynamic resistance $R_\mathrm{dyn} := dI/dU$ is practically zero or even slightly negative in case of

hydrogen discharges in the range $50 < I < 100\,\mathrm{A}$. A common (positive) resistor in series is therefore needed to stabilize the discharge. For technical reasons we were limited to $R \leq 0.3\,\Omega$ which turned out to be a bit marginal.
In what follows we report on the occurrence and the transport of suprathermal electrons, how they can be blocked by material limiters and the mechanisms involved in charging the neutralizer plate. Three different diagnostic tools were used: avalanche photo diodes for optical investigations as well as Langmuir probes and a segmented neutralizer plate.

2. Experimental arrangement

2.1. Plasma generator PSI-2

The investigations were performed at the plasma generator PSI-2, a linear device based on a stationary current arc discharge whose plasma is radially confined by an axial magnetic field, cf. Fig. 1. The plasma parameters pertinent for this work are $T_\mathrm{e} \approx 5\,\mathrm{eV}$, $n_\mathrm{e} \approx 10^{18}\,\mathrm{m}^{-3}$ (see Fig. 7), magnetic field strength $B = 0.1\,\mathrm{T}$ and neutral pressure $p_\mathrm{TC} = 10^{-3} \ldots 10^{-1}\,\mathrm{Pa}$.

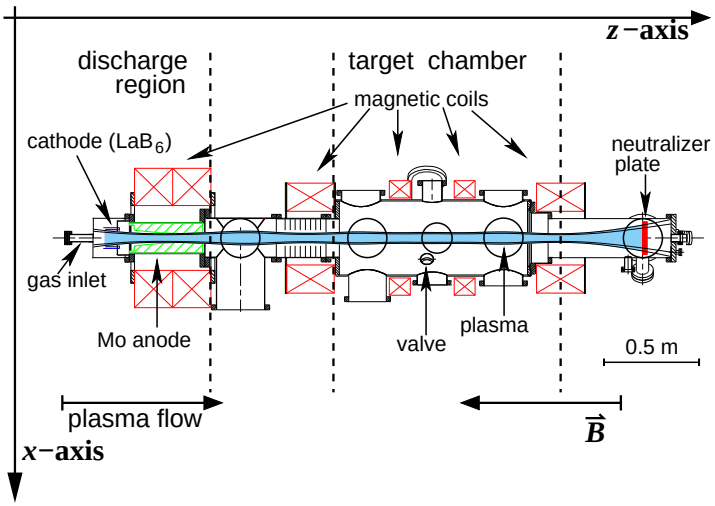

Figure 1. Plasma generator PSI-2.

Taking a closer look at the discharge region, cf. Fig. 2, reveals a thin circular ring structure which is of general importance with respect to the function of the device. It is determined by the inner and outermost radius of magnetic field lines hitting the cathode and passing the anode. It is this region where the highest electron density and temperature is found. As will be seen, it is also the region where the suprathermal electrons do appear.

2.2. Segmented neutralizer plate

In 2008 we developed a segmented neutralizer plate for the PSI-2 device [8, 9]. Instead of using a one piece plate, the segmented neutralizer plate is divided into ten rings and

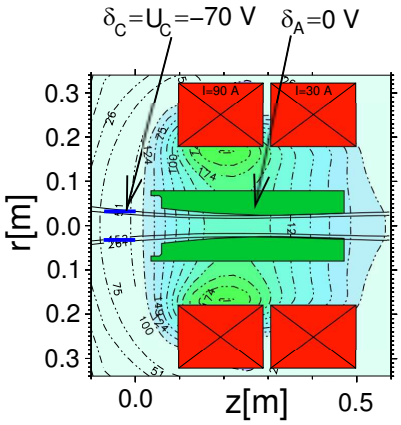

Figure 2. Discharge region. Cathode (blue), anode (green) and magnetic coils (red). The most inner and outer magnetic field lines hitting the cathode directly and passing the anode are indicated.

six sectors, each covering an angle of 60 °. An exception is the innermost ring which is divided into three sectors only. Thus, the segmented neutralizer plate consists of 57 isolated surface elements, all having a radial extension of 7 mm separated by a gap of 1 mm, cf. Fig. 3. Every single surface element can be biased and used as a Langmuir probe separately.

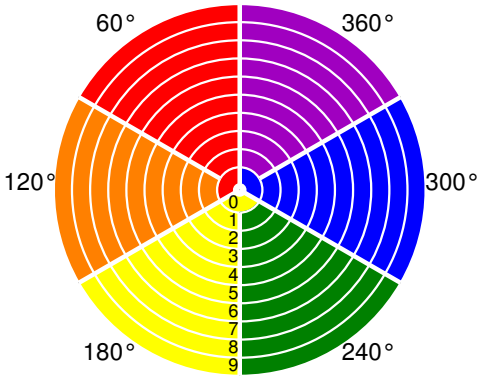

Figure 3. Segmented neutralizer plate [8].

3. Suprathermal electrons

3.1. Temporal course

We show a typical temporal course for a spike event in Fig. 4 (already presented in [1]). The cathode voltage (U_C) ‡ is suddenly enhanced by a factor of two (from −70 V to −140 V) within a time interval of about 1 μs. The same signature but delayed by 0.5 μs is found in the floating voltage of the unsegmented neutralizer plate (U_{np}) which covers the whole plasma cross section at the end of the discharge.

‡ All voltages are measured with respect to the grounded anode.

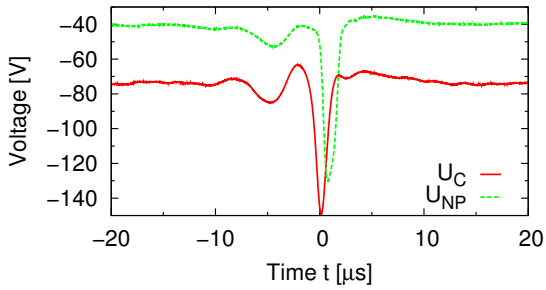

Figure 4. Voltage traces in a hydrogen discharge. Cathode voltage U_C and potential of the floating neutralizer plate U_np.

With the measured time of flight $\tau = 0.5\,\mu$s and the length $L = 2.8\,$m the velocity of the suprathermal electrons is calculated to $v_\mathrm{meas} = L/\tau = 5.2 \pm 0.2 \cdot 10^6\,$m/s. This value can be compared with the theoretical velocity of an electron that is accelerated in a short region close to the cathode where the major drop of the cathode-plasma voltage takes place: $v_\mathrm{theo} = \sqrt{-2e\,(U_\mathrm{C} - U_\mathrm{pl})/m_\mathrm{e}}$ with $U_\mathrm{C} = -145\,$V and a plasma potential of $U_\mathrm{pl} = -3.4\,k_\mathrm{B}T_\mathrm{e}/e \approx -17\,$V we estimate $v_\mathrm{theo} = 6.7 \cdot 10^6\,$m/s. The measured velocity is thus in fair agreement with the expected value.

3.2. Frequency of events

The spike events occur irregularly. We measured the frequency of events in dependence of the trigger voltage, cf. Fig. 5. There is an almost constant frequency of 60 Hz up to a peak level of $U_\mathrm{C} \approx 1.5 \cdot \langle U_\mathrm{C} \rangle$. For larger amplitudes, i.e. $|U_\mathrm{C}| > 135\,$V, one finds an exponential decay.

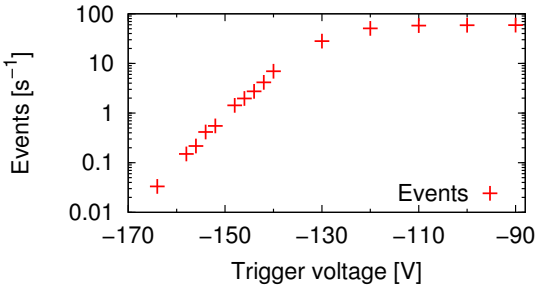

Figure 5. Frequency of events of suprathermal electrons with $\langle U_\mathrm{C} \rangle = -73\,$V on logarithmic scale.

To decide whether these electrons collide on their way through the plasma or can be treated as collisionless, the mean free path length has to be estimated. For electron collisions with electrons and ions the well known expressions (cf. [10])

$$\lambda_\mathrm{th} = \frac{9\pi\varepsilon_0^2}{e^4 \ln(\Lambda)} \frac{(k_\mathrm{B}T_\mathrm{e})^2}{n_\mathrm{e}} = 1.19 \cdot 10^{17} \frac{T_\mathrm{e}^2}{n_\mathrm{e} \ln(\Lambda)}\,[\mathrm{m}] \tag{1}$$

$$\lambda_\mathrm{st} = \frac{4\pi\varepsilon_0^2 m_\mathrm{e}^2}{e^4 \ln(\Lambda)} \cdot \frac{E_\mathrm{kin}^2}{n_\mathrm{e}} = \frac{4}{9} \frac{E_\mathrm{kin}^2}{(k_\mathrm{B}T_\mathrm{e})^2} \lambda_\mathrm{th} \tag{2}$$

are obtained from the basic relation $\lambda = v/(\nu_{ee} + \nu_{ei})$, in which E_{kin} is the kinetic energy of the electrons, ν_{ee} and ν_{ei} are the collision frequencies with thermal electrons and ions, respectively. $\ln(\Lambda)$, the Coulomb logarithm, is about 10 in the present context ($T_{e,th} \approx 5\,\mathrm{eV}$, $E_{kin} = 128\,\mathrm{eV}$ and $n_e \approx 1 \cdot 10^{18}\,\mathrm{m}^{-3}$).
It follows from the above equations for the thermal (subscript th) and the suprathermal (subscript st) particles:

$$\lambda_{th} \approx 0.26\,\mathrm{m} \qquad \text{and} \qquad \lambda_{st} \approx 170\,\mathrm{m}. \tag{3}$$

The mean free path length of the suprathermal electrons is hence by far larger than the length of the device ($L = 2.8\,\mathrm{m}$); they can be regarded as collisionless provided collisions with the neutral particles are sufficiently rare too, an aspect to be discussed in the following section.

4. Dependence on neutral gas density

In addition to the usual gas feed from the cathode end hydrogen was blown through a valve into the target chamber (cf. Fig. 1) to enhance the neutral density without interfering the discharge. The normal influx was $\Phi = 100\,\mathrm{sccm}$ § while the additional influx goes up as high as $\Phi_{add} = 175\,\mathrm{sccm}$. The discharge was not affected much, cf. p_{AC} and U_C in Fig. 6, while the neutral gas density in the target chamber p_{TC} rises and the floating potential of the neutralizer plate U_{np} is seen to decrease in the figure.

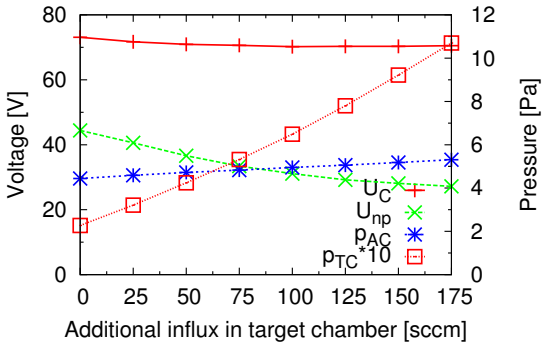

Figure 6. Various voltages and pressures as a function of the additional influx Φ_{add} into the target chamber.

A radially driven Langmuir probe measures the profiles of electron temperature T_e and density n_e. The additional gas cools the plasma thereby reducing volume ionization [11] which in turn results in a lower electron density, cf. Fig. 7. This process was misjudged in our prequel work [1].
The time of flight τ of the suprathermal electrons is seen to increase proportional to the neutral gas pressure, cf. Fig. 8, from $\tau(\Phi_{add} = 0\,\mathrm{sccm}) = 470\,\mathrm{ns}$ over $\tau(125) = 640\,\mathrm{ns}$ up to $\tau(175) = 730\,\mathrm{ns}$ while the peak area decreases.

§ Note: 1 sccm (standard cube cm per minute) is equivalent to a flux of $4.17 \cdot 10^{17}$ particles per second.

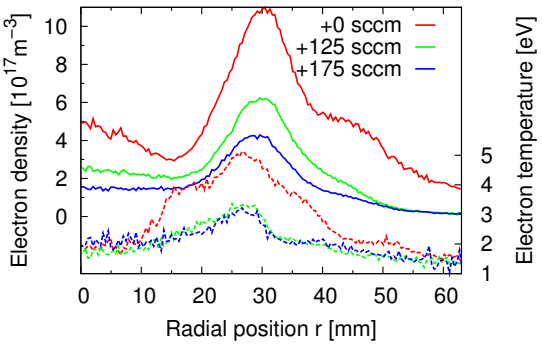

Figure 7. Radial n_e (solid lines) and T_e (dotted lines) profiles with the additional gas influx as a parameter. The flux in the discharge region was kept constant at $\Phi = 100\,\mathrm{sccm}$.

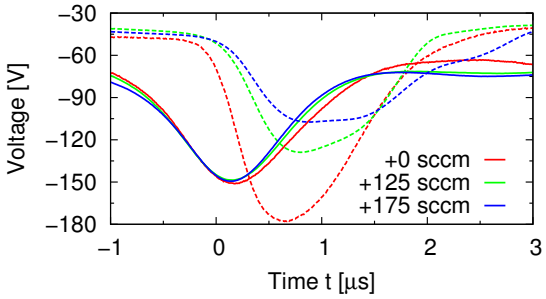

Figure 8. Temporal course of discharge voltage U_C (solid lines) and potential of the floating neutralizer plate U_{np} (dashed lines) in dependence of additional gas influx.

The assumption of non-collisionality is seen to break down and the collisions between suprathermal electrons and neutral gas have to be taken into account. The density of neutral hydrogen molecules n_{H_2} can be found from the conservation of particles

$$\frac{dN}{dt} = \Phi - \frac{N}{\tau_{\mathrm{pump}}}, \tag{4}$$

with Φ as the particle influx, τ_{pump} the confinement time given by the pumping rate S. For methane $\tau_{\mathrm{pump}}(CH_4) = 90\,\mathrm{ms}$ was measured [12]. Assuming that the pumping time depends on the inverse pumping rate of the turbo molecular pumps which itself depends on the square root of the mass of the species [13], it follows $\tau_{\mathrm{pump}}(H_2) \approx \frac{S_{CH_4}}{S_{H_2}} \cdot \tau_{\mathrm{pump}}(CH_4) = 255\,\mathrm{ms}$. The volume of the plasma chamber is $V = 0.33\,\mathrm{m}^3$, which leads to stationary molecular densities ($n = N/V$) of

$$n_{H_2}(\Phi_{\mathrm{add}} = 125\,\mathrm{sccm}) \approx 4.3 \cdot 10^{19}\,\mathrm{m}^{-3} \tag{5}$$

$$n_{H_2}(\Phi_{\mathrm{add}} = 175\,\mathrm{sccm}) \approx 6.0 \cdot 10^{19}\,\mathrm{m}^{-3}. \tag{6}$$

The suprathermal electrons are elastically scattered due to the polarisation of the hydrogen molecules with a cross section of $\sigma_{\mathrm{el}} = 5 \cdot 10^{-21}\,\mathrm{m}^2$ at an energy of $E \approx 160\,\mathrm{eV}$ [14]. This reduces the mean free path lengths to $\lambda(\Phi_{\mathrm{add}} = 125\,\mathrm{sccm}) = \frac{1}{\sigma_{\mathrm{el}} n_{H_2}} \approx 4.7\,\mathrm{m}$ and $\lambda(\Phi_{\mathrm{add}} = 175\,\mathrm{sccm}) \approx 3.4\,\mathrm{m}$. The latter value exceeds the length of the plasma only by 20%.

For a quantitative treatment the elastic scattering frequency

$$\nu_{\mathrm{el}} = n_{\mathrm{H_2}} \sigma_{\mathrm{el}} v. \tag{7}$$

is the relevant quantity. Elastic scattering leads to a diffusion in velocity space where, due to the big difference in masses ($m_{\mathrm{e}} \ll m_{\mathrm{H_2}}$), the magnitude of the velocity vector is an invariant. The scattering can be described by a diffusion equation akin to the Fokker-Planck-equation for the distribution function f

$$\frac{\partial f}{\partial t} = -\nabla_v \cdot \vec{\Gamma}_v = \nu_{\mathrm{e}} \frac{\partial}{\partial \mu}(1-\mu^2)\frac{\partial f}{\partial \mu} \tag{8}$$

in which $\vec{\Gamma}_v$ is a flux density in velocity space and $\mu = \cos(\theta) = v_z/v$ is the cosine of the scattering angle. The equation can be solved in spherical coordinates by an expansion in Legendre polynomials. The details of the calculation are reported in Appendix A. We chose $f(t=0,\theta) = \delta(\theta)$ as initial condition. To calculate the fraction of electrons reaching the neutralizer plate n_{np} one has to integrate $f(t,\theta)$ over the scattering angle $0 \le \theta \le \pi/2$. In the collisionless case ($\nu_{\mathrm{el}} = 0$) one obtains $n_{\mathrm{np}} = 1$ and in the isotropic case ($\nu_{\mathrm{el}} t \gg 1$) $n_{\mathrm{np}} = 1/2$. The average of the axial velocity is obtained to $\langle v_z \rangle = v\langle \mu \rangle = v \exp(-2\nu_{\mathrm{e}} t)$. Using this result the average path length $\langle z \rangle = \int_0^t \langle v_z \rangle \, dt$ is found to be $\langle z \rangle = \frac{v}{2\nu_{\mathrm{e}}}(1 - \exp(-2\nu_{\mathrm{e}} t))$. Putting $\langle z \rangle = L$ we then get the following relation for the mean time of travel

$$t = -\frac{1}{2\nu_{\mathrm{e}}} \ln\left(1 - \frac{2\nu_{\mathrm{e}} L}{v}\right) = t_0(1 + \nu_{\mathrm{e}} t_0 + \ldots) \tag{9}$$

with $t_0 = L/v$. Eq. (9) allows us to determine the collision frequency and hence the neutral density by inserting the experimental delay times on the left hand side. Taking the data from Fig. 8: $t_0 = t(\Phi_{\mathrm{add}} = 0) = 470\,\mathrm{ns}$, $t(\Phi_{\mathrm{add}} = 125\,\mathrm{sccm}) = 640\,\mathrm{ns}$ yields $\nu_{\mathrm{el}}(\Phi_{\mathrm{add}} = 125\,\mathrm{sccm}) = 7,7 \cdot 10^5\,\mathrm{s}^{-1}$. Similarly, $t(\Phi_{\mathrm{add}} = 175\,\mathrm{sccm}) = 730\,\mathrm{ns}$ results in $\nu_{\mathrm{el}}(\Phi_{\mathrm{add}} = 175\,\mathrm{sccm}) = 1,2 \cdot 10^6\,\mathrm{s}^{-1}$. From Eq. (7) we then receive with $v(E = 160\,\mathrm{eV}) = 7 \cdot 10^6\,\mathrm{m/s}$

$$n_{\mathrm{H_2}}(\Phi_{\mathrm{add}} = 125\,\mathrm{sccm}) = 2.2 \cdot 10^{19}\,\mathrm{m}^{-3} \tag{10}$$

$$n_{\mathrm{H_2}}(\Phi_{\mathrm{add}} = 175\,\mathrm{sccm}) = 3.4 \cdot 10^{19}\,\mathrm{m}^{-3}, \tag{11}$$

which is in rough agreement with the estimates given in Eq. (5) and (6).
For the largest additional flux ($\Phi_{\mathrm{add}} = 175\,\mathrm{sccm}$) we get from the measurement $t/t_0 = 1.55$ and therewith from eq. (9) (or eq.(A.11)) $\nu_{\mathrm{e}} t = 0.48$. Inserting this into eq. (A.8) yields for the number of suprathermals arriving at the neutralizer plate a ratio of $n_p(\Phi_{\mathrm{add}} = 175)/n_p(\Phi_{\mathrm{add}} = 0) = 0.78$. Comparing with the experimental data shown in Fig. 8 we notice that the influence of the collisions has been rather underestimated this way since the area included by the curves is seen to reduce to approximately 1/2.

5. Radial distribution

The importance of the mapped field lines was already mentioned in Sec. 2. The segmented neutralizer plate allows us to verify a radial constraint of the suprathermal

electrons. To this end we recorded the floating potentials of different segments triggered by the peaks in the cathode voltage U_C. The peaks at the inner and outer most radii are small and not correlated with the cathode voltage signal because of too large delay times: $|\Delta t| > 1.0\,\mu$s. Around the circular ring of the mapped cathode the peaks are more pronounced and correlated with the U_C peak voltage ($\Delta t = 0.2 \ldots 1.0\,\mu$s) cf. Fig. 9.

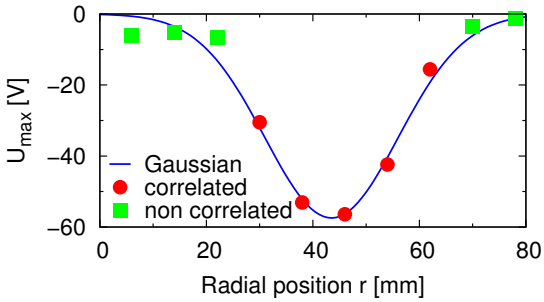

Figure 9. Voltage peaks of the floating neutralizer plate vs. radius.

A Gaussian was fitted to the data having its minimum at $r \approx 45\,$mm and a FWHM of 25 mm.

To ascertain whether the suprathermal electrons really follow the field lines after being released from the cathode, a radially driven Langmuir probe was set to different positions while a limiter was used to block the direct connection between the discharge region and the probe, cf. Fig. 10.

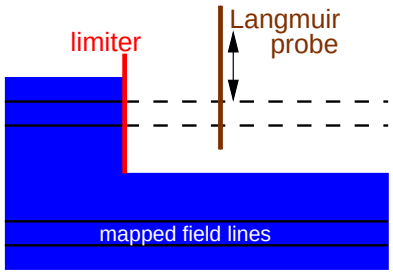

Figure 10. Radially driven Langmuir probe behind a limiter. The mapped field lines originating from the hollow cathode are also indicated. Plasma flows from left to right.

The Langmuir probe measured the fluctuating floating potential ($U_{\mathrm{fl}} - \langle U_{\mathrm{fl}} \rangle$). This was done with and without limiter at different radial positions (Fig. 11). Significant peaks were found at $r = 27\,$mm without limiter and in the undisturbed part of the limited plasma. This radial position coincides with the cathode mapped along the field lines. The distance between the limiter and the Langmuir probe was $\Delta z = 752\,$mm. The shadow of the limiter is marked in gray in Fig. 11. The strong reduction of the fluctuating potential is a clear indication that the limiter absorbs the suprathermal electrons. Further investigations using additional masks were reported in [15].

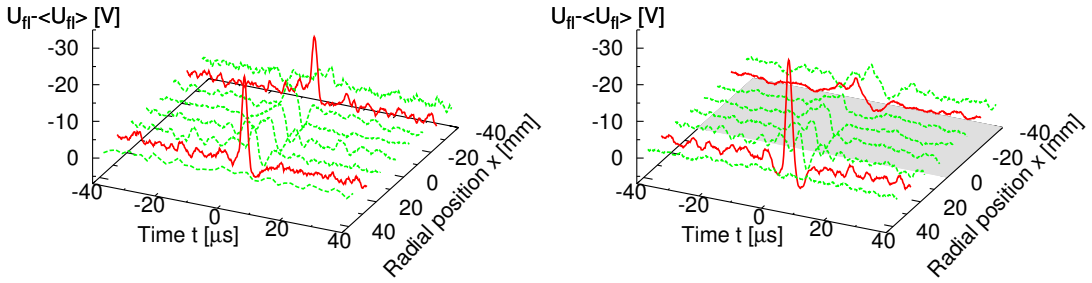

(a) Without Limiter (b) With Limiter

Figure 11. Fluctuating floating potential at different radial positions without (a) and with (b) limiter. Significant peaks are found at $r = 27\,\mathrm{mm}$. The limiter blocks the plasma in the half space $x < 0$ (shadow marked in gray). The axial distance between limiter and probe is $\Delta z = 752\,\mathrm{mm}$.

6. Charging of the neutralizer plate

6.1. Voltage overshooting at the neutralizer plate

Quite regularly it happens that the peak voltage measured at the neutralizer plate (vs. grounded anode) is larger in magnitude than the primary one at the cathode. Fig. 12 shows an example where U_C reaches a minimum of $-115\,\mathrm{V}$ while $0.5\,\mu\mathrm{s}$ later a voltage minimum of $U_\mathrm{np} = -135\,\mathrm{V}$ is measured on the radial surface element of the segmented neutralizer plate which is connected with the cathode along the magnetic field lines.‖

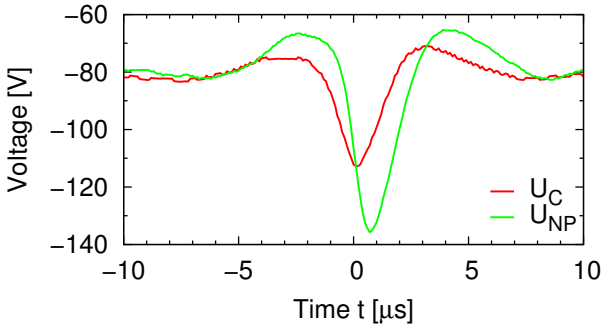

Figure 12. Voltage pulses at the cathode (red) and at neutralizer plate (green). ($I_\mathrm{plas} = 100\,\mathrm{A}$) [9].

This observation rises the fundamental question of whether it is compatible with energy conservation. Obviously, the maximum energy that single electrons gain by passing the cathode-anode region is 115 eV, but to charge the neutralizer plate to the observed voltage one is inclined to postulate that at least a minority would need an energy of 135 eV or higher. This conclusion is correct for continuous charging by single electrons

‖ Note that both voltages coincide about $\pm 10\,\mu\mathrm{s}$ before and after the pulses ($2\,\mu\mathrm{s}$ halfwidths) at a level of $-80\,\mathrm{V}$. This agreement is indicative of the high electrical conductivity of the plasma connecting the cathode and the collecting surface on the segmented neutralizer plate. The voltages differ when the neutral flux is enhanced but always stay much closer as in case of a uniform plate (see e.g. Fig. 4).

but fails when a large number of electrons is suddenly released from the cathode. In this latter case screening of the particles is important, enforcing a velocity distribution. Moreover, a temporary excess of the voltage at the neutralizer plate is possible, too. This can be shown explicitly by treating the problem in 1D approximation. Unfortunately, the complete derivation is too lengthy to be presented in this paper and will be published elsewhere. Here it may suffice to report the essentials: The whole temporal behavior can be subdivided into four different phases: During the initial phase $0 \leq t \leq t_1 = L_{\mathrm{AP}}/v_0$ with $v_0 = \sqrt{2eU_{\mathrm{C}}/m_{\mathrm{e}}}$ and L_{AP} = anode-plate distance, the electrons move towards the plate and at the time t_1 the most rapid ones arrive there. This period is followed by the actual charging phase $t_1 \leq t \leq 2t_1$ when the particles are absorbed at the surface. During the subsequent depletion phase $2t_1 \leq t \leq 4t_1$ the reflected particles move back to the cathode. Thereafter, during the stationary phase, the neutralizer plate potential is in fact on the cathode level, but prior, in particular during the charging phase, it is typically a factor 2 (at $t = t_1$) to 1.5 (at $t = 2t_1$) higher.

6.2. A two capacitor model

Despite the simplicity of the arrangement, the rigorous treatment of the problem – even in 1D – turned out to be quite demanding from the mathematical point of view. It is therefore profitable to discuss the physics by invoking an even simpler model consisting of two coupled capacitors. In fact, the geometrical arrangement can be regarded as comprising of a cathode-anode capacitor linked to a second one consisting of the anode and the neutralizer plate. They exhibit the capacities C_1 and C_2, respectively. The first one is initially loaded to voltage U_1, thus carrying the charge $Q_1 = C_1U_1$. By contrast, the second capacitor is initially unloaded, $Q_2 = U_2 = 0$.

First, we want to discuss the case when the two capacitors are connected by a resistor R. Then, a current $I = (U_1 - U_2)/R$ will flow, transporting charge from capacitor 1 to capacitor 2. The exchange of charge will vanish ($I = 0$) when both capacitors have attained the same voltage $U_1' = U_2' = U$. This final voltage can be inferred from the conservation of charge $C_1U_1 = C_1U + C_2U$ yielding $U = C_1U_1/(C_1 + C_2)$. Clearly, energy is not conserved when performing the charge transfer in this way, since ohmic heat is produced in the resistor. The amount of dissipated energy can be easily calculated by considering the stored electrostatic energies at the beginning $E = C_1U_1^2/2$ and at the end of the procedure $E' = (C_1 + C_2)U^2/2$.

Let us now consider the case where we manage to transfer the charges by satisfying both, charge conservation $C_1U_1 = C_1U_1' + C_2U_2'$ and energy conservation $C_1U_1^2/2 = C_1U_1'^2/2 + C_2U_2'^2/2$. Apart from the trivial solution $U_2' = 0, U_1' = U_1$ the two equations are satisfied by

$$U_2' = \frac{C_1}{C_1 + C_2} 2U_1 = 2U \qquad U_1' = \frac{C_1 - C_2}{C_1 + C_2} U_1 \tag{12}$$

In the case $C_2 \ll C_1$ we thus get $U_2' = 2U_1$ in agreement with our findings for the initial charging phase mentioned above. Note that during this phase energy is in fact

conserved since the particles filling the capacitor 2 already have not penetrated yet into the surface of the neutralizer plate. During the subsequent dissipation phase the voltage at the neutralizer plate was found to decrease down to the cathode level, again in agreement with the result found above assuming dissipative charging.
Finally, it should be mentioned that two plate capacitors (with a ratio of $C_2/C_1 = L_{\mathrm{CA}}/L_{\mathrm{AP}} \approx 0.1$, and L_{CA} the cathode-anode distance) do not appropriately describe the real configuration in PSI-2 under plasma conditions. Instead, the ratio $C_2/C_1 = 2U_{\mathrm{C}}/U_{\mathrm{np}} - 1 = 0.7$ inferred from the measured voltage ratio of $U_{\mathrm{C}}/U_{\mathrm{np}} = 1.17$ appears quite reasonable.

6.3. Voltage course including plasma reaction

So far we considered the charge transfer under vacuum conditions. The common voltage attained at the end of the charging period then simply depends on the amount of the total charge available and the capacities involved. This changes completely under plasma conditions because of the prevailing currents related to the thermal electrons and ions that tend to establish floating potential on all isolated surfaces. Taking these plasma currents into account the total current density reads

$$j = j_{\mathrm{e}} + j_{\mathrm{i}} + j_{\mathrm{st}} \;=\; j_{\mathrm{sat,i}}\left[1 - \exp\left(\frac{e(U_{\mathrm{np}} - U_{\mathrm{fl}})}{k_{\mathrm{B}}T_{\mathrm{e}}}\right)\right] + j_{\mathrm{st}} \tag{13}$$

in which j_{st} is the contribution of the suprathermals, $j_{\mathrm{sat,i}} = ec_{\mathrm{s}}n_{\mathrm{i}}/2 = en_{\mathrm{i}}\sqrt{k_{\mathrm{B}}(T_{\mathrm{e}} + T_{\mathrm{i}})/4m_{\mathrm{i}}}$ the ion saturation current density and U_{fl} the floating potential for $j_{\mathrm{st}} = 0$. The current density changes the surface charge $j = d\sigma/dt$ and, because of $E_z = \sigma/\varepsilon_0$ and $U_{\mathrm{np}} = E_z l$, we obtain the relation

$$\frac{\varepsilon_0}{j_{\mathrm{sat,i}}l}\frac{dU_{\mathrm{np}}}{dt} - \left[1 - \exp\left(\frac{e(U_{\mathrm{np}} - U_{\mathrm{fl}})}{k_{\mathrm{B}}T_{\mathrm{e}}}\right)\right] = \frac{j_{\mathrm{st}}}{j_{\mathrm{sat,i}}}\,. \tag{14}$$

The distance over which the potential changes from plasma to floating potential in front of the plate (the electrostatic sheath) is about four Debye lengths: $l = 4\lambda_D = 4\sqrt{\frac{\epsilon_0 k_{\mathrm{B}}T_{\mathrm{e}}}{e^2 n_{\mathrm{e}}}}$. Introducing $y = e(U_{\mathrm{np}} - U_{\mathrm{fl}})/k_{\mathrm{B}}T_{\mathrm{e}} < 0$ as a dimensionless variable, Eq. (14) takes on the form

$$\frac{1}{2\omega_{\mathrm{pi}}\sqrt{1 + T_{\mathrm{i}}/T_{\mathrm{e}}}}\frac{dy}{dt} - (1 - e^y) = \frac{j_{\mathrm{st}}}{j_{\mathrm{sat,i}}}, \tag{15}$$

in which the inverse of the ion plasma frequency $\omega_{\mathrm{pi}} = \sqrt{e^2 n_{\mathrm{i}}/\epsilon_0 m_{\mathrm{i}}} = 1.31\sqrt{n_{\mathrm{i}}\,[\mathrm{m}^{-3}]}\,[\mathrm{s}^{-1}]$ defines the characteristic time scale for relaxation to floating potential when the distortion (j_{st}) is switched off. For the relevant density $n_{\mathrm{i}} = n_{\mathrm{e}} = 10^{18}\,\mathrm{m}^{-3}$ we get $\omega_{\mathrm{pi}} \approx 10^9\ \mathrm{s}^{-1}$ whereas $dy/dt \approx y/\tau_{\mathrm{p}} \approx y10^6\ \mathrm{s}^{-1}$. The derivative term on the left hand side of Eq. (15) is hence typically of order $y/1000$ and therefore negligible in general. The resulting quasi-stationary solution $(1 - e^{y(t)}) = -j_{\mathrm{st}}(t)/j_{\mathrm{sat,i}}$ describes the situation when the suprathermal current replaces an equal amount of the thermal electron current which is suppressed by pushing the plate potential more negative. However, because of $(1 - e^y) < 1$ the quasi-stationary solution is applicable only if $-j_{\mathrm{st}}/j_{\mathrm{sat,i}} < 1$. In the

opposite case, $-j_{\rm st}/j_{\rm sat,i} > 1$, the derivative term in Eq. (15) is needed to satisfy the equation. Due to the large denominator a drastic increase of the plate potential (y) is then to be expected. This is exactly what the numerical solution of Eq. (15) presented in Fig. 13 shows.

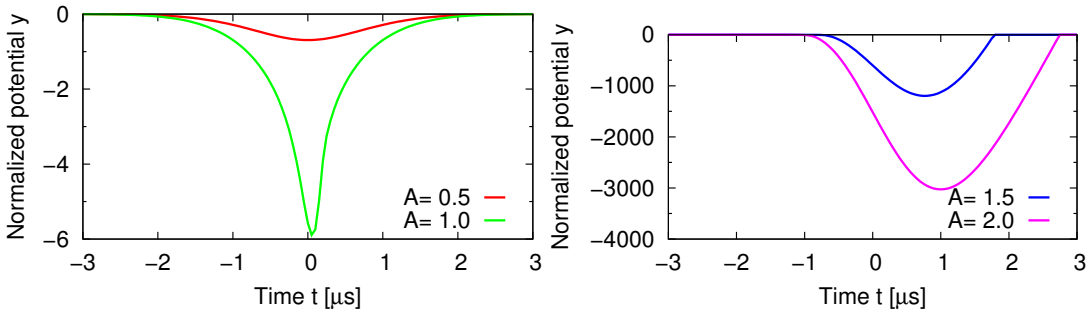

(a) (b)

Figure 13. Numerical solutions of Eq. (15) for the normalized potential y assuming $j_{\rm st}/j_{\rm sat,i} = A\exp(-(t/\tau_{\rm p})^2)$ with $\tau_{\rm p} = 1.2\,\mu$s and $\omega_{\rm pi} = 10^9\,{\rm s}^{-1}$. The amplitude A was chosen to (a): $A = 0.5$ (red), 1 (green) and (b): $A = 1.5$ (blue) and 2 (pink). Notice the drastic rise of y for $A > 1$.

6.4. Suprathermal current and particle densities

The calculations presented in the previous section allow us furthermore to determine the magnitude of the suprathermal currents prevailing in the experiments. With $k_{\rm B}T_{\rm e} = 5\,{\rm eV}$ (see Fig. 7) and $(U_{\rm min} - U_{\rm fl}) = -55\,{\rm V}$ the peak value of the normalized potential is obtained to $y_{\rm min} = -11$. Numerically this calls for a ratio of $j_{\rm st}/j_{\rm sat,i} = -1.01$. Actually, any value in the range $-y = 6$ to about 50 would yield a ratio very close to unity and this seems quite a reasonable result: As long as the suprathermal current can be compensated by the current of the ions the voltage changes are moderate. Larger suprathermal currents, however, are accompanied by a drastic fall of the plate potential, which in turn would rapidly cause a reflection of the suprathermals, too. This reflection is not accounted for in Eq. (15) but even so it is an effective control mechanism in reality. With the conclusion $j_{\rm st} = -j_{\rm sat,i}$ we are also in the position to determine the density of the suprathermals:

$$\frac{n_{\rm st}}{n_{\rm e}} = \frac{c_{\rm s}}{2v_{\rm st}} = \frac{1}{2}\sqrt{\frac{k(T_{\rm e}+T_{\rm i})/m_{\rm i}}{2e(U_{\rm C}-U_{\rm pl})/m_{\rm e}}} = \frac{1}{2}\sqrt{\frac{8}{2\cdot 90\cdot 1836}} = 2.5\cdot 10^{-3}\ . \quad (16)$$

On temporal average their influence is even much smaller: $\langle n_{\rm st}\rangle = n_{\rm st} f \tau_{\rm p}$. With the frequency of occurrence $f = 1\,{\rm s}^{-1}$ and $\tau_{\rm p} = 2\,\mu$s we get

$$\frac{\langle n_{\rm st}\rangle}{n_{\rm e}} = 5\cdot 10^{-9}\ . \quad (17)$$

This ratio is sufficiently small to ignore their existence in almost every respect.

7. Optical measurements

Besides the electrical measurements we also used avalanche photo diodes (APD) to detect the infrared emission at different axial positions. Because of the small fraction of the suprathermals compared to the thermal electrons (cf. Eq. (16)) the optical signal is a weak ac signal, indicative of the produced bremsstrahlung, but superposed by a strong dc signal of the thermal electrons. The ADP detector has a response time in the sub-μs range. We used one detector at different positions in a large number of measurements applying the cathode voltage signal for triggering and reference. To correct for delays in the transmission system the emission signal from the cathode is used to define the initial time $t = 0$ at all positions. The intensity pulses measured this way resemble very much the voltage pulses but are slightly broader and shifted in time. Fig. 14 shows the times of maximum emission at five different positions in comparison with the voltage maxima at the cathode and the neutralizer plate.

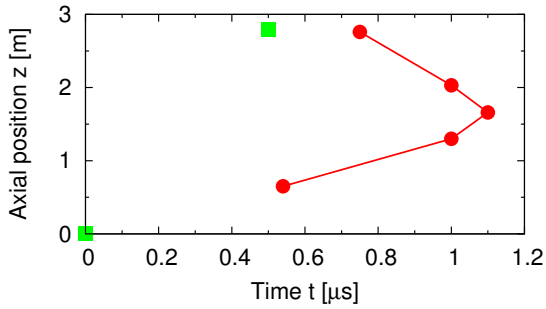

Figure 14. Times of maximum infrared intensity at various positions (red dots). The peak voltage times at cathode and neutralizer plate are also indicated (green squares).

First, we notice a good agreement for the times of arrival at the neutralizer plate: both, electrical and optical signals attain their peak values there after approximately $t = 0.5$ μs. Most surprising, however, is the fact that the optical signals at half the distance become maximal after almost twice this time, i.e. $t = 0.95$ μs.
Trying to understand this rather strange observation we have analyzed the dynamics of the suprathermal particles taking the voltage course at their place of birth, the cathode, into account. The voltage pulse at this position is approximately described by $U_C(t_0) = -U_0 \exp(-t_0^2)$ with t_0 in units of μs. The velocity of a particle released at time $t = t_0$ is then determined to $v(t_0) = \sqrt{-2eU_C(t_0)/m_e}$. Assuming that the emission current density is given by the *Child-Langmuir-law*, $j = -en_{st}v \propto |U_C|^{3/2}$ (see [16]), we infer for the particle density at the cathode $n_{st}(0, t_0) \propto |U_C(t_0)|$. Taking the time of flight into account the normalized density $\hat{n} = n_{st}/n_{max}$ at any position z is then obtained from

$$\hat{n}(z, t) = \hat{U}(t_0) \tag{18}$$

where the time t_0 is to be calculated from

$$\sqrt{\hat{U}(t_0)}\ (t - t_0) = z/v_{max}. \tag{19}$$

Here $\hat{U} = -U_C/U_0$ is the normalized voltage and $v_{max} = \sqrt{2eU_0/m_e}$. Eq. (19) can have none, one or two solutions. In the later case the starting times $t_0 = t_{1,2}$ can be both negative or one negative, the second positive.
A crucial point is the reflection of the particles at the neutralizer plate which brings in a third (negative) solution when replacing z by $z' = (2L - z)$ in Eq. (19). How this may explain the occurrence of the delayed maximum at $z = L/2$ shown in Fig. 14 shall be elucidated by means of a simple example. To this end we simplify the cathode voltage signal by a sum of three delta functions: $-\hat{U}_C(t_0) = 0.25\ \delta(t_0 + 0.5) + \delta(t_0) + 0.25\ \delta(t_0 - 0.5)$. Here the pre- and the post-courser, moving at half the velocity of the central pulse, are shifted by ± 0.5 μs. At $t = 0.5$ μs pre-courser and the central pulse arrive simultaneously at the neutralizer plate because of $L = v_0\ 0.5 = 0.5\ v_0\ (0.5 + 0.5)$. Let us further assume that the high energy central pulse is absorbed there whereas the low energy pre-pulse is reflected. Moving back towards the cathode it meets the post-courser at $z = L/2$ at $t = 1\mu$s, this time because of $L/2 = 0.5\ v_0(1 - 0.5) = 0.5\ v_0(0 + 0.5)$.
The preceding example may help us to conceive how a relative density maximum of the suprathermals can emerge earlier at the plasma end than at mid range. Quantitatively, however, it is not as easy to reconcile measurement and theory. This is because the true (full half) width of the voltage pulse is not 1μs, as assumed, but rather 2μs. In fact, a more detailed study, based on the equations given above, reveals that the assignment $v(t_0) \propto U_C^{1/2}(t_0)$ yields too broad a velocity function and a more rapid decrease of the velocity with decreasing voltage would be required. One possible mechanism operating in this direction is pitch angle scattering of the suprathermals that gains importance with decreasing speed and which has been found already pertinent at higher neutral density.

8. Conclusion

The existence of suprathermal electrons in a stationary arc discharge was confirmed by different diagnostic methods. First of all, evidence was given by peaks in the cathode voltage which could also be found with a temporal delay in the floating potential of the neutralizer plate terminating the plasma column. Secondly, they show up as fluctuations in the floating potential of a radially driven Langmuir probe. This way the region of their occurrence could be identified as a thin circular tube defined by the magnetic field lines originating from the ring-like cathode; its radial extension could also be identified by means of a segmented neutralizer plate.
The suprathermal electrons are blocked by material limiters but otherwise pass the plasma collisionless for low pressure conditions. Increasing the neutral gas pressure the assumption of non-collisionality fails and the electrons are scattered by the neutral background gas.
The suprathermals could also be substantiated in the plasma region from local measurements of the infrared bremsstrahlung produced by interaction with the ions. However, the times of maximum emission do not show a monotonous increase with

respect to the distance from the cathode. This observation seems to support the assumption that a major fraction of the suprathermals is reflected from the neutralizer plate.

For certain conditions the peak voltage of the floating neutralizer plate attains higher absolute values than the peak voltage of the cathode. This surprising observation is explained as a transient phenomenon occurring when a large number of electrons is suddenly released from the cathode. The underlying physics was elucidated by referring to a simple system of two capacitors in series. For the interpretation of the measured voltage signals the reaction of the plasma turned out to be most important. From a quantitative analysis we learnt that the current pulses of the suprathermal electrons are limited by the ion saturation current. As a consequence, we found that the peak density of the suprathermals is of order 10^{-3} compared to the thermal bulk electrons. On temporal average their concentration is further reduced and becomes as small as $10^{-8} n_\mathrm{e}$. For this reason we conclude that suprathermal electrons of the type found in PSI-2 are ignorable in general although they could be important with respect to excitation and ionization of higher charge states from a principle point of view.

Acknowledgments

We wish to express our gratitude to André Meißner for the design and conceptional analysis of the segmented neutralizer plate, to Siegfried Mettchen for all mechanical engineering regarding this plate and to Hans-Joachim Mans for supporting the optical measurements. It is gratefully acknowledged that Ekkekhard Pasch lent us the APD detector.

Appendix A. Elastic scattering of electrons at polarized molecules

In this appendix we present the derivation of Eq. (8) that describes the elastic scattering of the electrons caused by polarization of the molecules. The scattering can be described analogous to the Fokker-Planck-equation

$$\frac{\partial f}{\partial t} = -\nabla_v \cdot \vec{\Gamma}_v = \nabla_v \cdot (D_\mathrm{el} \nabla_v f) \tag{A.1}$$

where f is the distribution function. Here the subscript v assigns operators in velocity space and D_el is a diffusion coefficient in this space. The elastic scattering is a pure angular scattering from the original z-direction, which simplifies the right hand side of the equation. In spherical coordinates $\cos\theta = v_z/v$ it reads

$$\frac{\partial f}{\partial t} = D_\mathrm{el} \left(\nabla_v^2 f\right)_\theta = \frac{D_\mathrm{el}}{v^2} \frac{1}{\sin\theta} \frac{\partial}{\partial\theta} \left(\sin\theta \frac{\partial f}{\partial\theta}\right). \tag{A.2}$$

Substituting $\cos\theta = \mu$ and $\frac{D_\mathrm{el}}{v^2} = \nu_\mathrm{el}$, the collision frequency, it follows

$$\frac{\partial f}{\partial t} = \nu_\mathrm{el} \frac{\partial}{\partial\mu} \left(1-\mu^2\right) \frac{\partial f}{\partial\mu}. \tag{A.3}$$

This equation is solved by

$$f(\mu,t) = \sum_{l=0}^{\infty} a_l P_l(\mu) \exp\left(-l(l+1)\nu_{\rm el}t\right), \tag{A.4}$$

with P_l as the Legendre polynomial of l-degree. Choosing a delta function in z-direction $f(\mu,0) = \delta(\mu-1)$ as initial condition determines the coefficients a_l. Taking the orthogonality

$$\int_{-1}^{1} P_n(x)P_m(x)dx = \frac{2}{2n+1}\delta_{nm} \tag{A.5}$$

and the completeness

$$\delta(y-x) = \sum_{n=0}^{\infty} \frac{2n+1}{2} P_n(y)P_n(x) \tag{A.6}$$

properties of the Legendre polynomials, as well as $P_n(1) \equiv 1$, into account, we receive $a_l = (2l+1)/2$ and Eq. (A.4) becomes:

$$f(\mu,t) = \sum_{l=0}^{\infty} \left(l+\frac{1}{2}\right) P_l(\mu) \exp\left(-l(l+1)\nu_{\rm el}t\right). \tag{A.7}$$

If $\nu_{\rm el}t \gg 1$, the sum reduces to the term $l=0$ and we get $f \approx 1/2$. To calculate the amount of electrons reaching the neutralizer plate we have to integrate over the scattering angle $\theta < \pi/2$:

$$\begin{aligned} n_{\rm np} &= \int_0^{\pi/2} f(\theta,t)\sin\theta d\theta \;=\; \int_0^1 f(\mu,t)d\mu \\ &= \sum_{l=0}^{\infty} \frac{(l+1/2)\sqrt{\pi}\exp\left(-l(l+1)\nu_{\rm el}t\right)}{2\Gamma(1-l/2)\Gamma(3/2-l/2)}. \end{aligned} \tag{A.8}$$

For the collisionless case ($\nu_{\rm el}=0$) one obtains $n_{\rm np}=1$ whereas for isotropic conditions ($\nu_{\rm el}t \gg 1$) $n_{\rm np}=1/2$ is found.

Knowing the average z-velocity $\langle v_z\rangle = v\langle\mu\rangle$ one can determine the neutral density from Eq. (7). With $\mu = P_1(\mu)$ and the orthogonality Eq. (A.5) it follows

$$\langle\mu\rangle = \int_{-1}^{1} f(\mu,t)\mu d\mu \;=\; \exp(-2\nu_{\rm el}t). \tag{A.9}$$

Within a time t the electrons will travel on average the distance

$$\langle z\rangle = \; v\int_0^t \langle\mu\rangle dt = \frac{v}{2\nu_{\rm el}}\left(1-\exp(-2\nu_{\rm el}t)\right). \tag{A.10}$$

Taking $\langle z\rangle = L$ and $t_0 = L/v$ for the case without collisions leads to

$$\frac{t}{t_0} = \; -\frac{1}{x}\ln(1-x) = 1+\frac{x}{2}+\frac{x^2}{3}+\frac{x^3}{4}\ldots \tag{A.11}$$

with $x = 2\nu_{\rm el}t_0$. This relation was used in Sec. 4 to determine the collision frequency.

References

[1] O. Waldmann and G. Fussmann. *ECA - EPS Proc.*, 30I:P–1.049, 2006.
[2] L. Conde, L. Leon, and L. F. Ibanez. *IEEE T. Plasma Sci.*, 25:548–552, 1997.
[3] N. Ohno et al. *Phys. Rev. Lett.*, 81:818–821, 1998.
[4] E. M. Hollmann et al. *Phys. Plasmas*, 8:3314–3320, 2001.
[5] A. Escarguel et al. *Plasma Phys. Contr. F.*, 49:85–93, 2007.
[6] D. Nishijima et al. *Phys. Plasmas*, 14(10):103509, 2007.
[7] N. Ezumi. *Contrib. Plasma Phys.*, 48:435–439, 2008.
[8] A. Meißner. Diploma thesis, Fachhochschule, Frankfurt am Main/Germany, 2008.
[9] M. Langowski. Diploma thesis, Humboldt University, Berlin/Germany, 2009.
[10] D. V. Sivukhin. *Rev. of Plasma Phys.*, 4:93, 1966.
[11] O. Waldmann, H. Meyer, and G. Fussmann. *Contrib. Plasma Phys.*, 47:692–702, 2007.
[12] G. Fussmann et al. Studies of hydrocarbon formation and redeposition in ITER-relevant divertor chamber conditions. Technical Report Technology Task TW4–TPP–TRIDEP, Max-Planck-Institute Plasma physics and Humboldt University Berlin, 2006.
[13] W. Umrath. *Grundlagen der Vakuumtechnik*. Leybold Vakuum GmbH, Cologne/Germany, 1997.
[14] J.-S. Yoon et al. *J. Phys. Chem. Ref. Data*, 37:913–931, 2008.
[15] O. Waldmann. PhD thesis, Humboldt University, Berlin/Germany, 2009.
[16] F. F. Chen. *Introduction to plasma physics and controlled fusion Vol.1: Plasma Physics*. Plenum Press, New York, 2nd edition, 1984.